Subsea Release of Oil & Gas – A Downscaled Laboratory Study Focused on Initial Droplet Formation and the Effect of Dispersant Injection

Per Johan Brandvik
Dr. Scient., Senior Scientist/Professor
+47 9095 8576
per.brandvik@sintef.no

Øistein Johansen
oistein.johansen@sintef.no

Umer Farooq
umer.farooq@sintef.no
SINTEF Materials and Chemistry, NO-7465 Trondheim, NORWAY

Downloaded from http://meridian.allenpress.com/iosc/article-pdf/2014/1/283/1751252/2169-3358-2014_1_283.pdf by guest on 16 April 2024

ABSTRACT 300121:

This article describes the SINTEF Tower Basin (located in Trondheim, Norway) and its use for examining droplet formation and the effectiveness of dispersant injection. The Tower Basin is 6 m high and 3 m in diameter, containing 42 m^3 of natural sea water. Oil is injected from the base of the basin and oil droplets are monitored by laser diffraction and in-situ camera techniques.

Size distributions of oil droplets formed in deep water oil & gas blowouts have a substantial impact on the fate of the oil in the environment. However, very limited data on droplet size distributions from subsurface releases exist. The objective of this study has been to establish a laboratory facility to examine droplet size versus release conditions (flow rates and nozzle diameters), oil properties and injection of dispersants (injection techniques and dispersant types). Changes in the size of oil droplets that result from injection of dispersant are used to assess the effectiveness of the dispersant application (dosage and injection method).

This comprehensive dataset is used to develop and calibrate existing algorithms to predict droplet sizes from subsurface releases, and the effect of dispersant treatment. The improved algorithms are implemented in current operational models where they are used to describe subsurface use of dispersant and fate of the dispersed oil in the water column.

INTRODUCTION:

The size of oil droplets formed during a subsea release of oil and gas strongly influences the subsequent fate of the oil in the environment. Large droplets (larger than 5 mm) will reach the surface after a couple of hours rise time from a depth of 1000 m, while smaller droplets (down to 0.5 mm) may need up to a day before they will come to the surface. Finer droplets may stay in the water for weeks or months before they eventually reach the surface. However, factors like vertical turbulent mixing in the water column, density stratification and cross flows will contribute to keep such fine droplets submerged for even

prolonged periods (Johansen et al., 2003). These processes will also change the thickness and distribution of the resulting surface oil slick.

Reduction of oil droplet sizes is the primary rationale for subsea application of dispersants. Surfacing oil may have operational and safety impacts as well as environmental ones, since the presence of surface oil and resulting volatile components may hinder repair, mitigation, and other work in the vicinity of the wellhead.

The new SINTEF Tower Basin facility comprises a cylindrical water tank with a diameter of 3 m and a height of 6 m, containing about 42 m^3 of sea water (Brandvik et al., 2013). Trying to fully simulate a deep water, large-scale oil and gas blow-out in a 6-meter high basin is not possible. As such, we have focused on selected important aspects. These are scaled down and simulated in the Tower Basin (Johansen et al., 2013). The main objectives have been to study oil droplet size distribution as a function of:

1. Oil release conditions (nozzle diameter and release rates)
2. Different dispersant application techniques
3. Dispersant to oil ratios (DORs)

In recent and ongoing studies we have also focused on related topics including: Effectiveness of different dispersants, droplet coalescence and secondary droplet splitting, effect of oil temperature on droplet sizes and dispersant effectiveness and combined oil & gas releases. Publications based on results from these studies are in preparation.

Droplets in the Tower Basin are formed by turbulent breakup in the jet zone immediatelly after the release point (Hinze et al., 1955), where the oil/gas/water plume will quickly stabilize with respect to droplet the size distribution. The resulting plume will rise mainly due to the buoyancy of gas bubbles and oil droplets. As the plume rises, it also spreads laterally, increasing dilution with respect to distance from the release nozzle. Droplet measurements were performed in the centre of the plume approximately 2 metres above the release point to ensure sufficient dilution of the oil & gas plume.

The SINTEF Tower basin is considerably larger than tanks used in earlier studies. For example, Tang and Masutani (2003) used a tank with 0.5 by 0.5 m in cross section and 1.3 m in height, Neto et al. (2008) conducted their bubble breakup experiments in a tank with a width of 1.2 m and a height of 0.8 m. With this larger tank, droplet breakup experiments can be extended to higher flow rates (0.5 to 10 L/min) without the risk of saturating the water in the tank with dispersed oil droplets. A larger tank also facilitates the use of well-proven field and laboratory instrumentation for droplet size measurements that may be too large for use in smaller test tanks. The extensive oil droplet size distribution data generated in this facility have been used to derive a new model for prediction of oil droplet size distributions (Johansen et al., 2013).

This article presents the design of the test facility, results from studies with releases of oil, and demonstrates how simulated subsurface dispersant injection shifts the droplet size distribution toward smaller sizes.

Downloaded from http://meridian.allenpress.com/iosc/article-pdf/2014/1/283/1751252/2169-3358-2014_1_283.pdf by guest on 16 April 2024

EXPERIMENTAL:

An outline of the Tower Basin, showing the scaffolding/railing around the Tower Basin together with the ventilated hood and oil collecting system, is described and illustrated by Brandvik et al., 2013. An overview of the control system for oil, gas and dispersants is given in

Figure 1.

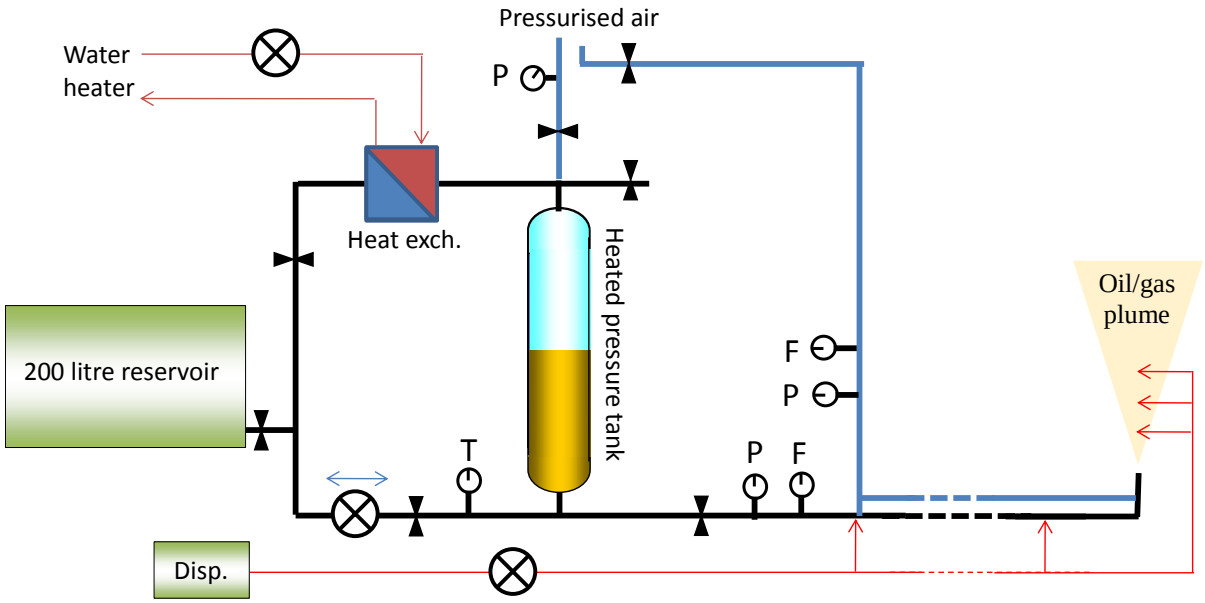

Figure 1: Principle overview of the set-up showing how oil, gas and dispersant are released during the experiments. The oil flow is controlled by pressurized air (P) and a mass controller (F). The dispersant is delivered by a high precision piston pump that is valved to several alternative injection pints. Gas flow is controlled by pressure (P) and a mass controller (F).

The oil flow rate is controlled by a mass flow controller and pressurizing the oil holding tank with Nitrogen. This system gives a pulse-free, reproducible and stable oil flow. At the most used flow rate (1.5 L/min), the documented variation is typically ± 0.015 L/min or 1%. Over multiple experimental replicates this variation in oil flow rate was found to have minimal influence on the measured droplet size distributions. The oil and water temperature ranges used in this study were 18-20 ºC and 8-10 ºC, respectively. The dispersant is delivered by a high precision piston pump to ensure controlled dispersant injection within the pressure range used to release oil (5 - 30 bars). The uncertainty in the flow rate delivered by the dispersant piston pump is ± 0.1% (1 -50 mL/min range). With the most frequently used dispersant rate of 15 mL/min (1.5 L/min oil and DOR of 1:100) this will introduce an uncertainty in the dispersant dosage of ± 0.0015 mL/min. This variation was documented by replicate experiments to have insignificant influence on the measured droplet size distributions. The gas is delivered from pressurized flasks through a mass flow controller with an uncertainty of ±1%. More details regarding the SINTEF Tower Basin are given by Brandvik et al., 2013.

Downloaded from http://meridian.allenpress.com/iosc/article-pdf/2014/1/283/1751252/2169-3358-2014_1_283.pdf by guest on 16 April 2024

Dispersant injection

A Teledyne Isco D1000 piston pump, with a range of 0.1- 408 mL/min and a maximum pressure of 120 bars, was used for dispersant injection. The dispersant can be injected in several different modes:

1. Upstream injection (3 meters before the release or 2000 nozzle diameters upstream with a 1.5 mm nozzle).
2. Simulated insertion tool. Dispersant injected 6 diameters before the release nozzle (see Figure 2-A1).
3. Injected into the rising oil plume (different distances above the nozzle), see Figure 2-A2.
4. Injected horizontally into the rising plume (different distances away from the plume or nozzle, see Figure 2-B).

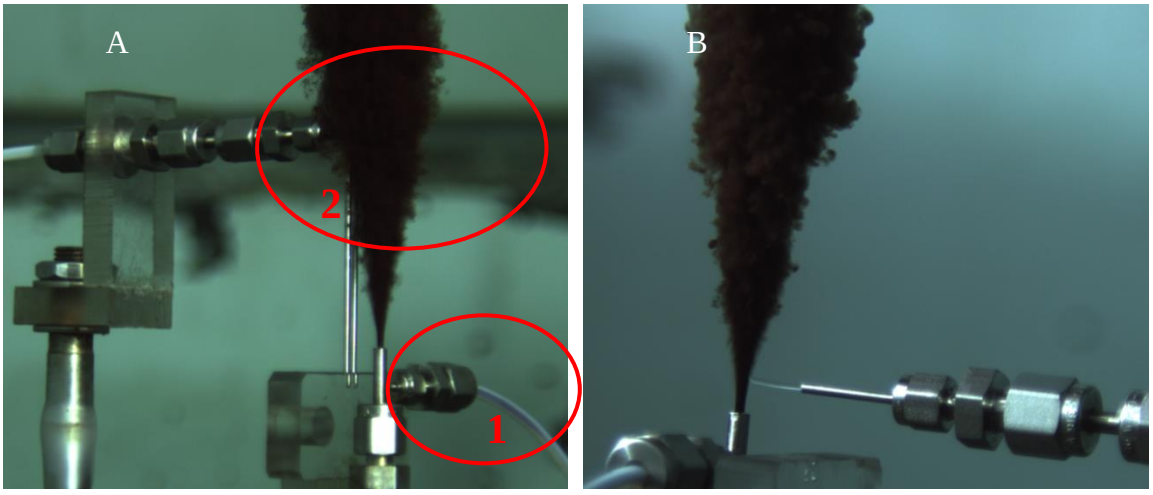

Figure 2: Release arrangement (1.5 mm nozzle) with options for injection of dispersant by "Simulated insertion tool" (A1) and "injection above the nozzle" (A2). Injection of dispersant horizontally into the oil is shown in B.

The surfactants in the dispersant orient themselves on the interphase between water and oil and reduce the interfacial tension (IFT) between the two phases. This reduced IFT allows formation of smaller droplets at a given turbulence level. The different injection modes are used to study effectiveness of different strategies for dispersant injection on subsurface releases of oil. This is the main focus for ongoing studies and more comprehensive results will be presented in later publications.

Downloaded from http://meridian.allenpress.com/iosc/article-pdf/2014/1/283/1751252/2169-3358-2014_1_283.pdf by guest on 16 April 2024

Oil type and dispersant

The oil used in this study was the Norwegian Oseberg blend. This is a typical light paraffinic blend with low viscosity and high evaporative loss (see Table 1). The data are from earlier weathering studies at SINTEF (Resby and Wang, 2004). Only one type of dispersant was used in this study, Corexit® 9500A, supplied directly by Nalco.

Table 1: Crude oil properties for Oseberg blend.

	Oseberg blend ID-2012-0060
Specific gravity (kg/l)	0.8393
Pour Point (°C)	-24
Viscosity (mPas at 13 °C)	5
Asphaltene (wt%)	0.2
Waxes (wt%)	2.7
150 °C – Evap loss (vol%)	23
200 °C – Evap loss (vol%)	35
250 °C – Evap loss (vol%)	46

Interfacial tension (IFT) measurements

Oil/water samples were collected in 1-litre long-necked measuring flasks. Oil appeared as droplets in the water with size a distribution dependant on the DOR and method of dispersant application. Oil settled as a layer in the narrow neck of the bottle and was collected for IFT measurements after 36 hours. The settling time was important for including smaller droplets in experiments with high dispersant effectiveness, which needed a longer settling time. No homogenization or heating was done before the IFT measurements. All IFT measurements were conducted at 13ºC. IFT measurements, conducted by spinning drop method (Khehifa and So, 2009), were performed on the Dataphysics Spinning Drop Tensiometer SVT-20N with control and calculation software SVTS 20 IFT. Measurements were done on multiple droplets, where standard deviations were typically ± 0.2 for high IFT values (2-20 mN/m) and ±0.01 for low IFT values (0.01 – 2 mN/m). More details concerning the oil sampling and IFT measurements are given by Brandvik et al., 2013.

Monitoring of droplet size distributions

Monitoring of droplet sizes was performed in the centre of the plume approximately 2 metres above the release point to ensure sufficient dilution of the oil and gas plume A suite of instrumentation was mounted on a piston operated platform which is inserted into the plume. The platform was mounted on a slide attached to the inner wall of the basin, such that its vertical position could be continuously changed. Since documentation of oil droplet size distribution is central in this project, three different approaches are used to measure the droplet size distribution of the rising oil droplets:

a. The LISST-100X is a laser diffractometer for in-situ observations of particle size

Downloaded from http://meridian.allenpress.com/iosc/article-pdf/2014/1/283/1751252/2169-3358-2014_1_283.pdf by guest on 16 April 2024

distribution and volume concentration. It also records the optical transmission, pressure and temperature.

b. Custom made in-situ macro camera utilizing two green lasers for illuminating the plane of focus.
c. In-line Particle visual microscope (PVM).

The stream of images produced by the in-situ macro camera and the PVM were processed via image analysing software to produce droplet size distributions. However, for this set of experiments, the laser diffractometer (LISST-100X) was the main instrument used for particle analysis and this method is discussed in more detail below.

The laser diffraction instrument (LISST-100X) determines size distribution of an ensemble of particles and is operated in-situ in the Tower Basin. Laser diffraction is not strongly affected by the composition of particles because the scattering light recorded is within very small forward angles. At these small angles, light scattering is dominated by diffraction as opposed to the composition-sensitive refractive processes that are more influential at larger angles (Davies et al., 2012). Uncertainties due to shape or compositional effects are small in this study since the measured particles (oil droplets) are spherical and have identical composition since we are using the same oil type (Karp-Boss 2007 and Andrews et al., 2010, Graham et al., 2012).

Temperature gradients during the release (caused by releasing warm oil into cold water) are small and the effects of schlieren on the LISST response (Mikkelsen et al., 2008) have not been observed within the Tower Basin.

Attenuation of light across the sample volume of the LISST is both dependent on concentration and droplet sizes. If beam attenuation becomes too high, errors will result from multiple scattering effects (where scattered light from one droplet becomes incident on another). An optical path reducer (provided by the manufacturer) that restricts the optical path from 50 mm to 10 mm was used to extend the concentration range for the LISST instrument. The instrument was also operated two meters above the release point to obtain a suitable dilution of the oil plume (25-150 mg/L), but maintain a sufficient signal to noise ratio. For these reasons the applied laser diffraction methods deliver a size distribution of equivalent spherical diameters that is very suitable for quantifying oil droplets and gas bubbles in natural sea water, without disruption of the sample volume that is inevitable with ex-situ measurements.

The data presented in this paper are primarily obtained with the laser diffraction instrumentation (LISST-100X). Further details regarding this and the other two methods for droplet size determination can be found in Brandvik et al., 2013.

RESULTS:

The LISST instrument makes 10 measurements every second (covering 32 logarithmically spaced bins in the 5-500 µm range) and store these as an average reading. An average over a 30-second period, which means 300 individual droplet size distribution scans, is

Downloaded from http://meridian.allenpress.com/iosc/article-pdf/2014/1/283/1751252/2169-3358-2014_1_283.pdf by guest on 16 April 2024

used in this study to quantify each droplet size distribution. Averaging over this period should reduce uncertainties from possible drifting or pulsing of oil or dispersant flow rates and inhomogeneity in the rising oil plume. The system has been calibrated with a standard consisting of mono-disperse polypropylene particles (6, 20, 38, 80, 165 and 346 µm). To confirm correct size measurements, two of the mono disperse standards (80 and 346 µm) were always injected in front of the submerged LISST before each experiment was initiated in the Tower Basin.

In this study data near the lower limit of the droplet size range measured by the LISST (the first three size classes) have been omitted from the results due to measurement artefacts from presence of surfactant micelles when high dosages of dispersants are used.

We have chosen to define the characteristic droplet diameter as the centre of the bin where the maximum peak is observed in the distribution. If the droplet size distribution follows a lognormal distribution, this peak diameter will coincide with the volume median droplet size (VMD or d_{50}) within the uncertainty given by the finite bin size, but this may not be true for other distribution functions. More details regarding assumed distributions can be found in Johansen et al., 2013. For one of the datasets (d_{50} as a function of dispersant dosage), the cumulative d_{50} was used to discriminate between closely spaced distributions due to the relatively large bin sizes. For some of the distributions, where quantification of the largest droplets is not complete (see Figure 7), using the cumulative distribution will produce slightly underestimated values of d_{50}.

The results presented in this paper represent two types of experiments performed in the Tower Basin (see table 2):

1. Studies of initial droplet formation as a function of release diameter, flow rate and oil properties.
2. Studies of subsurface dispersant effectiveness

Table 2: d_{50} as a function of nozzle diameter, oil flow rate and dispersant to oil ratio (DOR). d_{50} is estimated from peak values in droplet size distributions measured with LISST instrumentation in SINTEF Tower Basin. Calculated release velocities (U) and measured IFTs are also given. IFTs were measured on oil samples collected from the oil plume in the Tower basin.
3.

Nozzle diameter (mm)	Oil flow rate (L/min)	Dispersant (DOR)	U (m/s)	IFT (mN/m)	d_{50} (µm)
0.5	0.10		8.5	15.5	186
0.5	0.20		17.0	15.5	88.2
0.5	0.50		42.4	15.5	27.7
1.5	0.50		4.7	15.5	390
1.5	1.2		11.3	15.5	237
1.5	2.8		26.4	15.5	104
3.0	2.0		4.7	15.5	460[1]
3.0	5.0		11.8	15.5	331
3.0	8.0		18.9	15.5	280
0.5	0.2	1:100	17.0	nd	32.7
0.5	0.2	1:50	17.0	nd	23.5

Downloaded from http://meridian.allenpress.com/iosc/article-pdf/2014/1/283/1751252/2169-3358-2014_1_283.pdf by guest on 16 April 2024

1.5	1.2		11.3	15.5	259
1.5	1.2	1:100	11.3	nd	88.2
1.5	1.2	1:50	11.3	nd	74.7
3.0	5.0	1:100	11.8	nd	128
3.0	5.0	1:50	11.8	nd	104
3.0	5.0	1:25	11.8	nd	74.7
1.5	1.2	1:1000	11.3	9.5	246[2]
1.5	1.2	1:500	11.3	2.9	207[2]
1.5	1.2	1:250	11.3	1.3	211[2]
1.5	1.2	1:100	11.3	0.7	171[2]
1.5	1.2	1:50	11.3	0.07	123[2]
1.5	1.2	1:25	11.3	0.08	71[2]

4. [1] Based on analysis of PVM images
5. [2] Based cumulative distributions
6. nd: Not determined

Droplet size distribution as a function of release diameter and flow rate

Experiments were performed with different nozzle sizes (0.5, 1.5 and 3 mm) and flow rates (0.1 – 8 L/min). The main objectives were: 1) to study initial droplet formation as a function of oil injection velocity into the water, and 2) to produce a data set to verify that our system design follows existing scaling laws for turbulent droplet breakup (Weber number scaling). The results are presented in Figure 3 where selected volume distributions for three different nozzle sizes and flow rates are shown. The results from the flow rate experiments are also presented in a scaled form together with data from an earlier study in Figure 4.

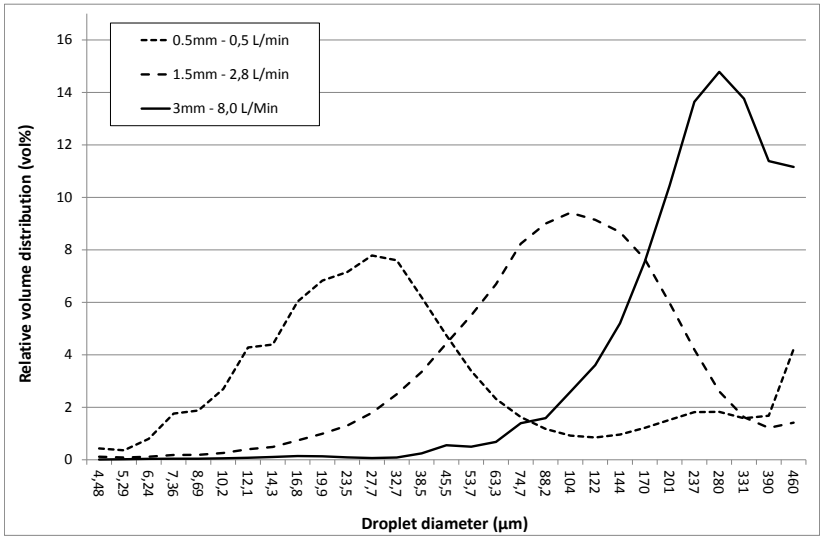

Figure 3: Relative droplet size distribution (volume %) as a function of nozzle size (0.5, 1.5 and 3 mm) and flow rate (0.5 – 8 L/min) for the Oseberg oil measured with LISST instrumentation in SINTEF Tower Basin.

Downloaded from http://meridian.allenpress.com/iosc/article-pdf/2014/1/283/1751252/2169-3358-2014_1_283.pdf by guest on 16 April 2024

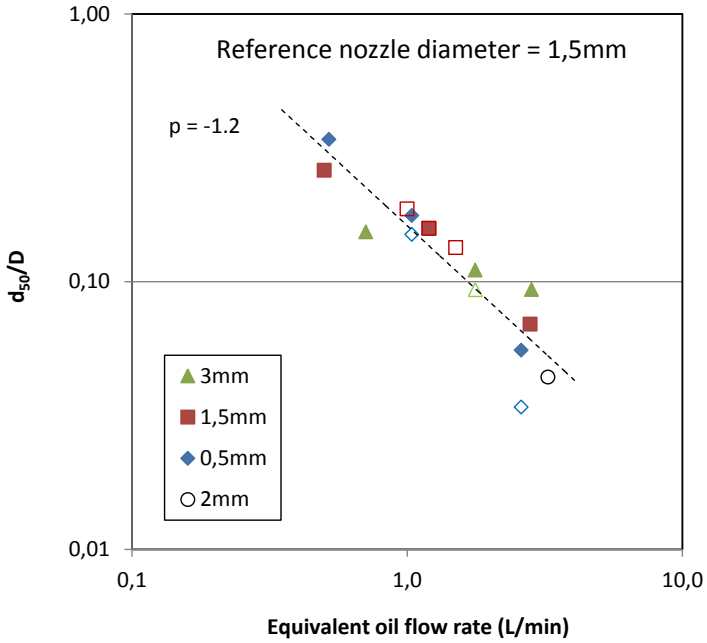

Figure 4: Results from the flow rate experiments presented in a scaled form together with additional data from Brandvik et al., 2013 (open symbols). The relative peak diameter d_P/D is plotted vs. equivalent oil flow rates (Q_a). The equivalent oil flow rate refers to an apparent fixed nozzle diameter of 1.5 mm (see equation 2).

Droplet size distribution as a function of dispersant injection

In general, droplet sizes are reduced when dispersant is injected into the oil flow, due to the reduction in interfacial tension (IFT) between oil and water. Figure 5 presents a series of experiments where the dispersant was injected into the oil jet six nozzle diameters above the release nozzle (0.5, 1.5 and 3.0 mm). The dispersant (Corexit 9500A) was injected at a DOR of 1:100 and 1:50. Data for these experiments are included in

Table 2.

Figure 6 shows the droplet size distributions for another dispersant injection technique where the dispersant is injected into the oil jet six diameters above the release nozzle (Figure 2). The droplet size distributions for, a third injection method (upstream injection) is presented in Figure 7. This figure presents the droplet size distributions as a function of dispersant dosage (DOR 1:1000 – 1:25). d_{50} values from Figure 5B, Figure 6 and Figure 7 are plotted together as a function of DOR in Figure 8. This figure compares d_{50} values for a 1.5 mm nozzle with three different dispersant injection techniques.

Downloaded from http://meridian.allenpress.com/iosc/article-pdf/2014/1/283/1751252/2169-3358-2014_1_283.pdf by guest on 16 April 2024

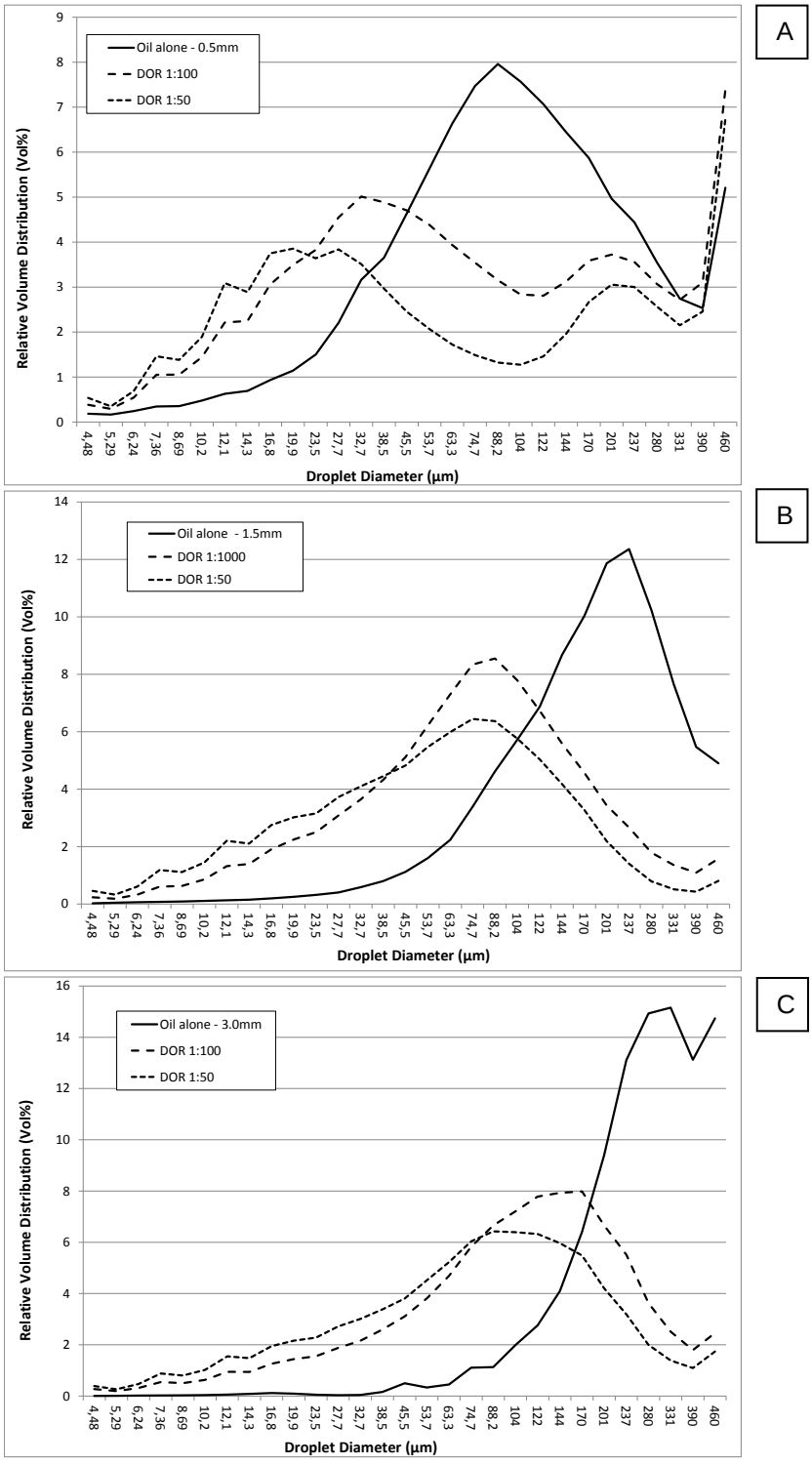

Figure 5: Relative droplet size distribution (volume %) with different nozzle sizes (0.5, 1.5 and 3 mm) dispersant injected 6 release diameters above nozzle. Dispersant Corexit 9500A and Dispersant to Oil Ratios (DOR: 1:100 and 50) with Oseberg oil measured with LISST instrumentation in SINTEF Tower Basin.

Downloaded from http://meridian.allenpress.com/iosc/article-pdf/2014/1/283/1751252/2169-3358-2014_1_283.pdf by guest on 16 April 2024

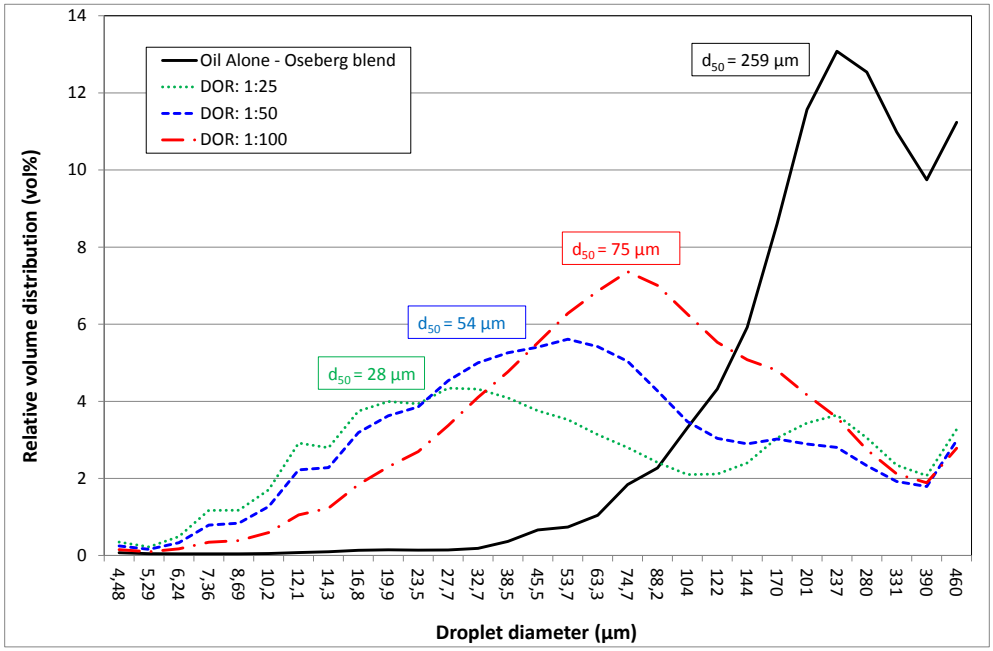

Figure 6: Relative droplet size distribution (volume %) with the simulated insertion tool with different Dispersant to Oil Ratio (DOR: 1:100, 50 and 25) on the Oseberg oil measured with LISST instrumentation in SINTEF Tower Basin. Release conditions 1.5 mm and 1.2 L/min.

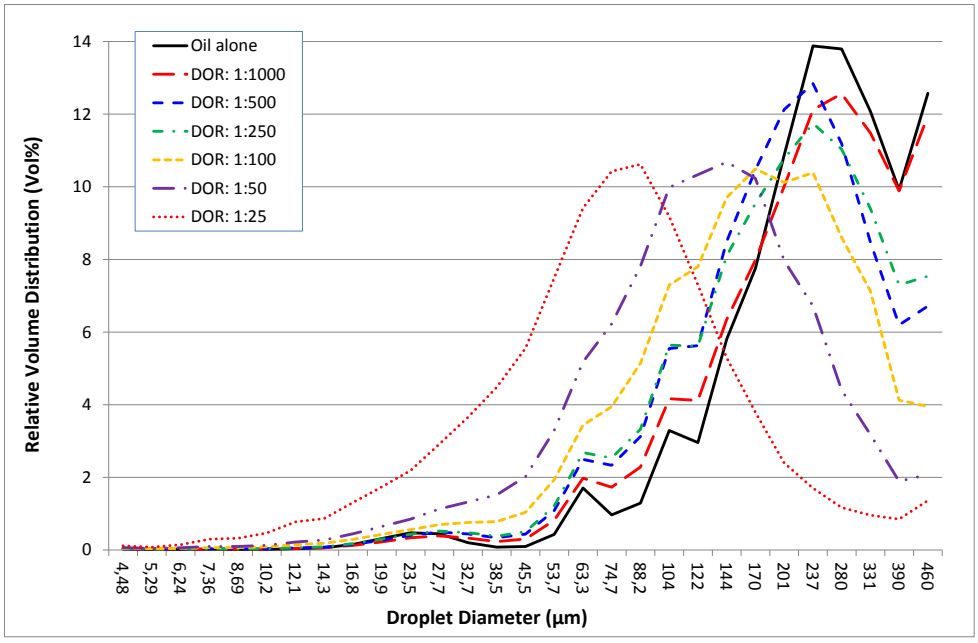

Figure 7: Relative droplet size distribution (volume %) as a function of Dispersant to Oil Ratio (DOR) with the Oseberg oil and Corexit 9500A measured with LISST instrumentation in SINTEF Tower Basin. Release conditions 1.5 mm and 1.2 L/min. Dispersant was injected by upstream injection.

Downloaded from http://meridian.allenpress.com/iosc/article-pdf/2014/1/283/1751252/2169-3358-2014_1_283.pdf by guest on 16 April 2024

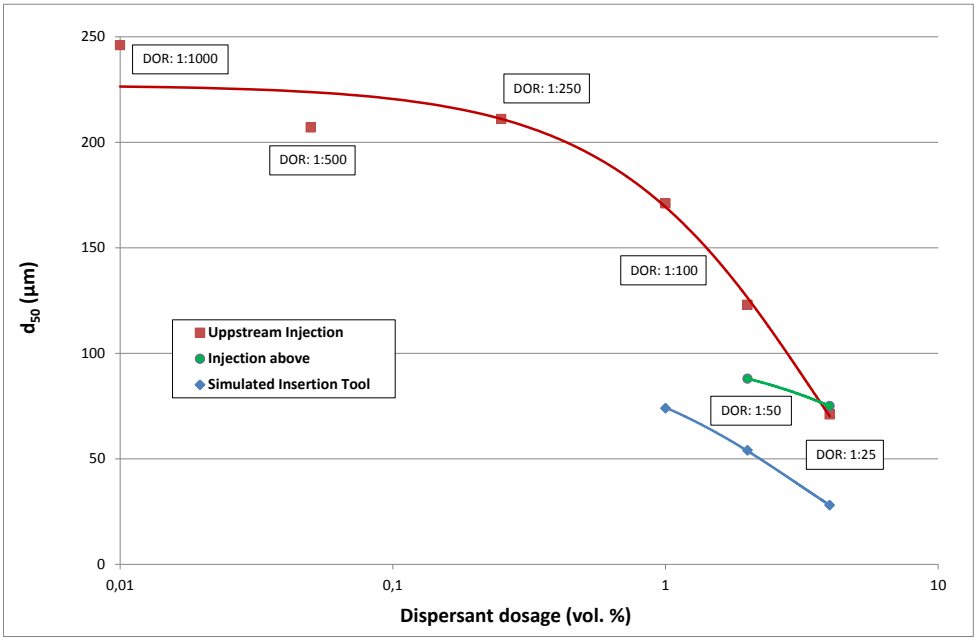

Figure 8: Volume Mean Droplet size (VMD) or D_{50} as a function of dispersant dosage. The dispersant is either injected upstream (red squares – data from Figure 7), 6 release diameters above the nozzle (green circles – data from Figure 5B) or 6 release diameters before (blue diamonds – data from Figure 6). Droplet sizes are measured with LISST instrumentation. Experimental conditions are 1.5 mm nozzle, Corexit 9500A and Oseberg blend.

DISCUSSION & CONCLUSIONS:

The data from the flow rate experiments cover a relatively wide range of nozzle sizes (0.5 – 3 mm) and flow rates (0.1 – 8 L/min). A shift towards smaller droplets with an increase in flow rate with constant nozzle diameter is presented in

Table 2 for three different nozzle sizes.

This variation in nozzle sizes and flow rate give release velocities over a wide range (5 - 42 m/s) and this data could therefore be used to look for possible underlying droplet breakup scaling laws. The theory for turbulent breakup of liquid jets points to a Weber number scaling law, expressed as:

$$d'/D = A\ \mathrm{We}^{-3/5} \qquad (1)$$

where d' is a characteristic droplet diameter, D is the nozzle diameter, A is a factor of proportionality and $\mathrm{We} = \rho U^2 D/\sigma$ is the exit Weber number, where ρ is the density of the liquid in the jet (oil) and σ is the interfacial tension (IFT) between oil and water. Since the flow conditions are defined by the nozzle diameter, D (m), and the oil flow rate, Q (m^3/s), in this study, it could be more convenient to express the Weber number in terms of these variables. This gives the following equivalent equation for the Weber number scaling law:

$$d'/D = A\ [(4/\pi)^2\ (\rho/\sigma)\ Q^2/D^3]^{-3/5} \qquad (2)$$

Downloaded from http://meridian.allenpress.com/iosc/article-pdf/2014/1/283/1751252/2169-3358-2014_1_283.pdf by guest on 16 April 2024

This implies that the relative characteristic droplet size d'/D should be equal for equal values of the scaling factor Q^2/D^3. This can be used to rescale the experimental data set for a range of oil flow rates to certain reference nozzle diameter (D_a). Equation 2 shows that the apparent flow rate for a reference nozzle diameter is $Q_a = Q\,(D_a/D)^{3/2}$.

Figure 4 shows a plot of the results from the flow rate experiments, scaled to a reference nozzle diameter (D_a =1.5 mm), together with a similar data set from Brandvik et al., 2013 (open symbols). The two datasets show a very good correlation. Broken lines show the expected slope for a Weber number scaling ($p = -3/5 \cdot 2 = -1.2$) for a fixed nozzle diameter of 1.5 mm. The good correspondence between the slope of this line and the scaled data points is a strong indication of an underlying Weber number scaling law. Some clear deviations from the line are found, but they may be explained as experimental uncertainties in either the accuracy of controlling low flow rates, or low resolution in determining the exact peak droplet size (due to large bin sizes from the LISST instrument).

Only the experiments without use of dispersant are included in Figure 4, since a simple Weber number scaling does not fit the data from the dispersant experiments (Brandvik et al., 2013).

Table 2 shows that the maximum reduction in peak droplet size, relative to the result without dispersant, is between a factor of 2-3, but a Weber scaling, based on a reduction in IFT from 15.5 mN/m without dispersants to < 0.1 mN/m for the highest DOR, should imply a reduction in droplet size by a factor of about 20 (equation 2). A reduction in droplet size by a factor of 2-3 is certainly significant, but the lack of correspondence with predictions from a simple Weber scaling law implies that other factors must limit droplet breakup in cases with significant reductions in IFT. A possible candidate is internal viscous forces, but these issues are discussed more in details in Johansen et al., 2013. Data from this and related studies are used to develop an improved algorithm for prediction of droplet size distributions from subsurface oil & gas releases (Johansen et al., 2013). This new algorithm (modified Weber number scaling) also includes dispersant injection and is implemented in operational oil spill models describing the fate of deep water oil & gas releases and the effect of dispersant injection (Johansen, 2003).

When dispersant is injected into the oil it lowers the IFT between oil and water (σ) and shifts the droplet size distribution towards smaller sizes (d'/D). This is illustrated in Figure 6 where dispersant (C9500A) is injected by simulated insertion tool (SIT) and d_{50} is shifted from 259 µm (oil alone), to 75, 54 and 28 µm for DORs 1:100, 1:50 and 1:25, respectively.

An important down-scaling criterion in this laboratory approach is the release diameter. Experiments were performed where dispersant was injected six release diameters above the release for three different nozzle sizes (0.50, 1.5 and 3.0 mm). The results, presented in Figure 5, show that dispersant treatment (DOR 1:100) gives a relative reduction in d_{50} of 0.34-0.38 for all three nozzles. This means that for all three nozzle sizes d_{50} is reduced to approximately a third at a DOR 1:100. This strengthens our confidence in using the release diameter as an important scaling factor.

To study the effect of different dispersant dosages the DOR is varied between 1:1000 and 1:25 with upstream injection in Figure 7. The figure indicates a limited effect of the

Downloaded from http://meridian.allenpress.com/iosc/article-pdf/2014/1/283/1751252/2169-3358-2014_1_283.pdf by guest on 16 April 2024

dispersant (reduction in droplet sizes) for the lowest dosages, but the 1:100 to 1:25 shows a significant shift towards smaller sizes. The low response detected by the peak in distribution could be masked by the relatively large bin sizes for the LISST instrument. If cumulative distributions are calculated, it is easier to show a trend in the material towards smaller droplet sizes. Figure 8 shows the cumulative d_{50} as a function of dispersant dosage and a clearer trend can be seen. The droplet data for the same nozzle size (1.5 mm) for two other injection techniques (Simulated insertion tool and Injection above nozzle) are also illustrated in the same figure. The limited data presented here indicate a difference between the injection techniques in their ability to reduce droplet sizes. Further details concerning this will be presented later where a more comprehensive dataset allows for more thorough analyses of these different injection techniques (Brandvik et al. in preparation).

Replicate experiments show that the experimental uncertainty in both the oil flow rate (1%), dispersant injection (0.1%) and quantification of oil droplet distributions are all low compared to the observed variation in droplet sizes due to release conditions (nozzle diameter and flow rate) and dispersant treatment. The largest source of uncertainty in this study is likely to be inhomogeneity in the oil-water-gas plume created in the tank. This is minimized by measuring droplet sizes in the same location for all experiments and averaging over a long period (30 seconds or 300 individual LISST measurements). Since no water is exchanged during an experiment in the Tower Basin, recirculation of old droplets could interfere with the LISST measurements. However, this is mainly a concern for the smaller droplets, due to their reduced rising velocity, and experiments are terminated before recirculation significantly influences the measured droplet size distributions. Experiments with untreated reference oil, performed initially and repeated at the end of each experiment, also show the same droplet size distributions.

The importance of the findings summarized in this article have encouraged continued investigations of oil droplet breakup with different injection methods, oil temperatures, presence of gas, different DORs, dispersant products and oil types. Results from this ongoing work are now being reported and the results will be published later. The projects performed so far in our Tower Basin have been focusing on the initial droplet formation from mixed release of oil and gas under turbulent jet conditions. Other processes like secondary droplets splitting could change the droplet size distributions after the initial formation as the droplets rise through the water column. These processes are currently not included in operational models used to describe deep water releases and could lead to overestimation of oil droplet sizes. However, several research projects are now been initiated to increase our knowledge regarding the behaviour of the droplets after the initial formation.

ACKNOWLEDGEMENT:

This study has been a part of a larger R&D project at SINTEF with the overall objective to increase our understanding of droplet formation during deep water oil & gas blow-outs and the effectiveness of subsurface dispersant injection. The data presented here are from a study financed by the American Petroleum Institute under contract 2012-106675. The experiments were performed during 2012. The authors would like to thank the technical staff at SINTEF for significant input to the success of this project, especially senior engineer Frode Leirvik for operating the tower basin.

Downloaded from http://meridian.allenpress.com/iosc/article-pdf/2014/1/283/1751252/2169-3358-2014_1_283.pdf by guest on 16 April 2024

REFERENCES:

Andrews, S., Nover, D. and Schladow, S.G., 2010: Using laser diffraction data to obtain accurate particle size distributions: the role of particle composition. Limnol. Oceanogr.: Methods 8, 2010, 507–526.

Brandvik, P.J., Johansen, Ø., Leirvik, F., Farooq, U., and Daling, P.S. 2013. Droplet breakup in sub-surface oil releases – Part 1: Experimental study of droplet breakup and effectiveness of dispersant injection. Mar. Pollut. Bull. 2013 Volume 73, Issue 1, 15 2013, pp. 319-326.

Davies, E.J., Nimmo-Smith, W.A.M., Agrawal, Y.C., and Souza, A.J. 2012. LISST-100 response to large particles. Mar. Geol. 2013 Volumes 307-310, pp. 117-122.

Graham, G.W., Davies, E.J., Nimmo-Smith, W.A.M., Bowers, D.G., Braithwaite, K.M., 2013, Interpreting LISST-100X measurements of particles with complex shape using digital in-line holography. Journal of Geophysical Research, 2012 Volume 117, C05034.

Hinze, J.O., 1955. Fundamentals of the hydrodynamic mechanism of splitting in dispersion processes. A.I.Ch.E. Journal, 1, 289-295.

Johansen, Ø., 2003. Development and verification of deep-water blowout models. Marine Pollution Bulletin, 47, 360-368.

Johansen, Ø., Rye H. and Cooper C., 2003. Deep Spill – Field Study of a simulated oil and gas blow-out in deep water. Spill Science & technology Bulletin, 8, 433-443.

Johansen, Ø., Brandvik, P.J., and Farooq, U. 2013. Droplet breakup in sub-surface oil releases – Part 2: Predictions of droplet size distributions with and without injection of chemical dispersants. Mar. Pollut. Bull. 2013 Volume 73, Issue 1, 15 2013, pp. 327-335.

Karp-Boss, L., Azevedo, L. and Boss, E. 2007: LISST-100 measurements of phytoplankton size distribution: Evaluation of the effects of cell shape. Limnol. Oceanogr.: Methods 5, 2007, 396–406.

Khelifa, A. and So L.L.C., 2009. Effects of Chemical Dispersants on Oil-Brine Interfacial Tension and Droplet Formation. 32nd AMOP Techn. Seminar, 383-396.

Mikkelsen, O.A., Milligan, T.G., Hill, P.S., Chant, R.J., Jago, C.F., Jones, S.E., Krivtsov, V. and Mitchelson-Jacob, G. 2008: The influence of schlieren on in situ optical measurements used for particle characterization. Limnol. Oceanogr.: Methods 6, 2008, 133–143.

Neto, I.E.L, Zhu, D.Z., and Rajaratnam, N., 2008: Bubbly jets in stagnant water. International Journal of Multiphase Flow. 34, 1130-1141.

Downloaded from http://meridian.allenpress.com/iosc/article-pdf/2014/1/283/1751252/2169-3358-2014_1_283.pdf by guest on 16 April 2024

Resby J.L.M. and Wang U.M. 2004: Update of weathering properties of Oseberg Blend, SINTEF Technical report STF80 F04015, pp. 7. PO box 4760 Sluppen, N-7465 Trondheim Norway.

Tang L., and S.M. Masutani, 2003: Laminar and Turbulent Flow Liquid-liquid Jet Instability and Breakup. Proceedings of the Thirteenth International Offshore and Polar Engineering Conference, Honolulu, Hawaii, USA, pp. 317-324.

Downloaded from http://meridian.allenpress.com/iosc/article-pdf/2014/1/283/1751252/2169-3358-2014_1_283.pdf by guest on 16 April 2024